



# Canadian Journal of Civil Engineering

## An experimental study on cyclic behaviour of RC connections using waste materials as cement partial replacement.

Journal:	<i>Canadian Journal of Civil Engineering</i>
Manuscript ID	cjce-2018-0555.R1
Manuscript Type:	Article
Date Submitted by the Author:	07-Nov-2018
Complete List of Authors:	Murad, Yasmin; University of Jordan, Civil Engineering Department Abu-Haniyi, Yousef; Dar Al-Handasah Alkaraki, Alaa; econstruct Hamadeh, Zeid; Adnan Hamadeh and partners co
Keyword:	pulverised fuel ash, silica fume, iron filling, cyclic, reinforced concrete connections
Is the invited manuscript for consideration in a Special Issue? :	Not applicable (regular submission)

SCHOLARONE™  
Manuscripts

# **An experimental study on cyclic behaviour of RC connections using waste materials as cement partial replacement**

First Author: Yasmin Murad, PhD., DIC.  
Assistant Professor  
Civil Engineering Department  
The University of Jordan  
Amman, Jordan 11942  
Phone Number: + 962-79- 6666802  
E-mail: [y.murad@ju.edu.jo](mailto:y.murad@ju.edu.jo)

Second Author: Yousef Abu-Haniyi, BSc  
Structural design engineer  
Dar Al-Handasah shair and Partners  
Amman - Jordan  
Phone Number: + 962-79-1516205

Third Author: Alaa AlKaraki, BSC  
Structural engineer  
econstruct  
Amman - Jordan  
Phone Number: +962796871392

Fourth Author: Zeid Hamadeh, BSc  
Junior Manager  
Adnan Hamadeh and partners co  
Amman - Jordan  
Phone Number: 00962777882858

## Abstract

A series of cyclic tests on unconfined beam-column connections with composite concrete materials are conducted. Cement is partially replaced by waste materials using two different percentages 15% and 20%. The proper percentage of cement replacement is found 15% for the Pulverized fuel ash, silica fume and iron fillings. Increasing the percentage to 20% tends to relatively decrease concrete compressive strength, weaken the joint and reduce its ductility.

It is recommended using pulverized fuel ash to enhance the performance of beam-column connections under cyclic loading. Silica fume and iron filling have also enhanced joint response but the enhancement is most remarkable when using 15% pulverized fuel ash. The implementation of composite concrete has increased joint's ductility and reduced its level of damage based on the type and percentage of the implemented waste material. Furthermore, the disposal of waste materials into concrete mix is a good solution for reducing environmental pollution.

## Keywords

Experimental, waste materials, pulverised fuel ash, silica fume, iron filling, cyclic, connections, ductility, reinforced concrete.

## 1. Introduction

Many existing reinforced concrete (RC) buildings are vulnerable to earthquake loads due to insufficient shear reinforcement in beams and columns, widely spaced column ties, and little or no transverse reinforcement within beam-column joint regions. Beam-column connections play a key role in integrating a whole structural system, thus any shear failure in beam-column connections may contribute to the collapse of a building.

In order to assess the performance of unreinforced beam-column joints which do not have transverse reinforcement, considerable research has been carried out over the last four decades to investigate the behaviour and failure mechanisms of RC beam-to-column connections. Experimental tests have been conducted and analytical models have been developed to describe the response of beam-to-column connections in RC planar frames under cyclic loading.

The parameters affecting the shear strength in RC connections are limited to the following: concrete strength, joint aspect ratio, bond resistance, beam longitudinal reinforcement ratio, column axial load, the characteristics of transverse beams, slab effects and joint transverse reinforcement. Therefore, changing the concrete strength can change the type of failure in beam-column connections.

Alternative damage failure mechanisms that can be developed in connections are illustrated in the literature (Murad 2016) such as J-failure, BJ-failure etc. J-failure is joint shear failure where pure shear failure happens in the joint core without forming any plastic hinges in beams or columns as shown in Figure 1 . Joint shear failure is a brittle failure where failure happens under relatively small rotations and the strength represents the actual shear strength of joints. BJ-failure denotes the type of failure which initiates by yielding of beam longitudinal reinforcement followed by joint shear failure. BJ failure mode is more ductile than J failure mode because of beam reinforcement yielding.

Various waste materials with different percentages have been commonly used to replace part of cement in concrete. These additives such as fly ash, silica fume, fuel ash, rice husk, iron filing and oil shale can enhance mechanical and durability characteristics of concrete and can be eliminated into the concrete mix. Researchers have conducted many experiments to find the proper percentage of cement replacement for each waste material. The percentage of replacement varies based on the adopted waste material type.

Previous studies (Khedr et al. 1994) showed that the flexural strength and compressive strength of silica-fume concrete were significantly improved. They suggested an optimum content of silica fume between 15% and 20% at which maximum strengths were obtained. They also reported that the elastic modulus, toughness, and steel-concrete bond were increased in silica- fume concrete.

Previous researchers (Liu 2010) showed that self-compacting concrete with up to 80% cement replaced by fly ash was possible. They recommended that ash can have negative effects on consistence retention and hardened concrete such as strength. Other researchers (Dhir et al. 1984) proposed that pulverised fuel ash concrete can achieve comparable strength to ordinary concrete at earlier ages, with much higher strengths at later ages.

In addition, previous tests (Lam et al. 1998) proposed that fly ash substantially can improve the post-peak compressive behaviour of concrete. It was also found that low volumes of fly ash improved the tensile strength of concrete while high percentage of fly ash decreased the tensile strength. They also reported that a small amount of silica fume had a large positive effect on the cylinder compressive strength and tensile strength but less on the cube compressive strength, while the fracture behaviour was brittle.

Previous experimental program (Alzaed 2014) was conducted for 144 standard cubes and cylinders using 0%, 10%, 20% and 30% of iron filing in concrete mix. The study showed that concrete compressive strength increased gradually with the increment of iron filing while the tensile strength did not change significantly with the increment of the filling. Other researchers (Noori et al. 2018) conducted tests to investigate iron waste effect on concrete.. Iron waste was used in different

percentages (6%, 12%, 18%, 24%, and 30%) as sand replacement. The test showed that 12% of iron waste was more efficient than the other percentages in both compressive and flexural strength while increasing iron waste to more than 12% decreased the strength of concrete.

**Figure 1 joint shear failure (Pampanin, Calvi, and Moratti 2002)**

Therefore, the implementation of composite concrete materials, which may have different compressive strengths, can change the behavior of beam-column sub-assemblages and their failure modes under cyclic loading. Composite concrete materials with high strength and ductility are capable of enhancing the behavior of RC beam-column connection under seismic loading.

## **2. Experimental Program**

### **2.1 Test objectives**

The aim of this project is to better understand the seismic performance of unconfined beam-column connection using composite concrete materials. Cement in concrete mix is partially replaced by different waste materials with different percentages to better understand the effect of composite concrete mixes on the seismic performance of unconfined beam-column connections. Composite mixtures that have different compressive strengths can change the behavior of RC beam-column sub-assemblages and their failure modes under cyclic loading. Composite concrete materials with high strength and ductility are capable of enhancing the behavior of RC beam-column connections under cyclic loading. This research proposes replacement percentages of cement with different waste materials and investigates the capabilities of composite concrete materials to enhancing the behavior of RC beam-column connections under seismic loading.

### **2.2 Materials and Methods**

Cement in concrete mix is partially replaced by different waste materials with different percentages. These materials such as fly ash, silica fume, fuel ash, rice husk, iron filing can enhance the properties of concrete depending on their percentages. Pulverized fuel ash, silica fume and iron filing are used in

this project as cement partial replacement. The cement replacement percentages adopted in this research for each material are 15% and 20%. Plane and recycled concrete mixing ratios are given in Table 1.

**Table 1 Plane and recycled concrete mixing ratios**

Pulverized fuel ash is a by-product of pulverized fuel (normally coal) resulting from fired power stations. The fuel is pulverized into a fine powder, mixed with heated air and burned. It is composed of fine particles that are driven out of the boiler with the fuel gases.

Silica Fume is an ultrafine powder collected as a by-product of the silicon and ferrosilicon alloy production. The main field of application is as pozzolanic material for high performance concrete.

Iron Filings are mostly a by-product of the grinding, filing, or milling of finished iron products, so their history largely tracks the development of iron. For the most part, they have been a waste product.

### **2.2.1 Material Properties**

Chemical composition of the implemented waste materials is shown in Table 2. Table 3 summarises the properties of the adopted waste materials. Waste materials, including pulverised fuel ash, silica fume and iron filling, are used as partial replacements of cement in concrete mixes in two different percentages 15 % and 20%.

**Table 2 Chemical composition of the implemented waste materials.**

**Table 3 Properties of the waste materials**

## **2.3 Specimen Details**

Eight 1/3-scale unconfined interior beam-column sub-assemblages are tested under cyclic loadings. The details of the test specimens are shown in Figure 2. The control specimens P-1 and P-2 are designed to promote joint shear failure at which failure should happen at joint while the longitudinal reinforcement in beams and columns should remain elastic. Cement, in concrete mixes, is partially replaced by 15% and 20% of silica fume in specimens S-15 and S-20 respectively. Specimens A-15, A-20, I-15 and I-20 contain 15% and 20% of pulverised fuel ash and iron fillings respectively as

partial replacements of cement in concrete mixes. The cylinder compressive and tensile strengths for all specimens are given in Table 4 and Table 5 respectively where the strength is taken as the average of two specimens for each concrete mix. The average longitudinal and transverse reinforcement yield strengths are 420 MPa and 280 MPa, respectively. Curing time is 120 days. The specimens are instrumented to measure global response, applied loads, joint shear strains as shown in Figure 3. The constraints of specimens and the applied lateral load pattern are illustrated in Figure 4.

**Table 4 Specimens' compressive behaviour**

**Table 5 Specimens' tensile behaviour**

**Figure 2 Test specimen details**

**Figure 3 Test setup**

**Figure 4 (a) Specimens constraints and (b) lateral load pattern**

## **2.4 Test setup**

The test setup consists of lateral loading system, and lateral restraint system as shown in Figure 3 and Figure 4. Column is pinned from the bottom end only while the ends of the beams are pin connected allowing horizontal translation from one end only as shown in Figure 3. A hydraulic actuator is connected to the top of the column to apply lateral load by means of a loading collar. A quasi-static cyclic load is applied at the column top and measured using a load cell which is located between the hydraulic actuator and the loading collar. The actuator is pinned at the end to allow rotation during the test. Lateral loads are applied as force-controlled steps beginning at  $\pm 5$  kN load followed by load increments of 5 kN at each cycle up to a maximum load of 55kN at cycle 11 as shown in Figure 4. The load application speed is 2kN/min.

Two high-accuracy strain gauge displacement sensors, which implemented to measure joint shear strain, are fixed at the joint face along its diagonals, as shown in Figure 5. Strain gauge length is 2 mm which is very small. This can reduce the chance of crossing strain gauges by cracks. Furthermore, the experimental program compares between the behaviors of test specimens that are made from different composite concrete materials and tested under the same level of loading. Experimental strains are recorded until cycle 11 ( $\pm 55$ kN), although the specimens can sustain greater lateral loads. Thus, joint



panel has not been damaged significantly reducing the chance of crossing strain gauges by cracks. Therefore, strain gauges are able to measure joint deformation until cycle 11 without any interruption.

**Figure 5 Strain gauges location**

## 2.5 Joint panel response

Joint response is expressed in terms of the joint shear stress and shear strain and it is also expressed in respect of the normalized joint shear stress and shear strain. This section illustrates the definitions of joint shear stress and strain.

### 2.5.1 Joint shear stress

Paulay and Priestley (Paulay and Priestley 1992) defined the horizontal shear force across the joint region  $V_j$  in interior connections as shown in Equation 1:

$$V_j = C_b + T_b - V_c \text{ (for interior connections)} \quad \text{Equation 1}$$

Where

$C_b$ : Beam compression force which is the sum of the compression forces in concrete  $C_c$  and in reinforcement  $C_s$ .

$T_b$ : Beam tensile force.

$V_c$ : Column shear force.

A simplified way to calculate the joint shear force  $V_j$ , based on the joint geometry and the lateral force  $V_c$ , is adopted in this paper. Equation 2 was proposed by Matsumoto et al. (Matsumoto et al. 2012) to calculate the experimental joint shear force. The symbols given in Equation 2 for joint geometry are illustrated in Figure 2.

$$V_j = \left\{ \left( \frac{l_b - h_c}{j_d} \cdot \frac{l_c}{l_b} \right) - 1 \right\} V_c \quad \text{Equation 2}$$

Where

$l_b$  is the total beam span length

$h_c$  is the column depth.

$l_c$  is the total column height

$j_d$  is the assumed moment arms at both beam-column interface ( $j_d = 0.9 d$ )

The normalized joint shear stress is defined as illustrated in Equation 3

$$\tau_j = \frac{V_j}{b_j h_c \sqrt{f'_c}} \quad \text{Equation 3}$$

Where

$b_j$  is the effective joint width as defined in ACI-352R-02 (ACI 352 2002).

$f'_c$  is concrete compressive strength

The ACI-352-02 (ACI-352 2002) defines the nominal joint shear strength in (MPa) for modern beam-column connections as shown in Equation 4. The ACI-352-02 formulation is adopted in this paper to predict joint shear strength. The predicted ultimate joint shear stress is calculated as:  $\frac{V_j}{b_j h_c}$ .

$$V_j = \gamma \sqrt{f'_c} b_j h_c \quad \text{Equation 4}$$

$\gamma$  is the joint shear strength factor provided in MPa<sup>0.5</sup> that depends on joint classification and is taken as 1.67 based on ACI-352-02 (ACI-352 2002) for the interior joints tested in this paper.

### 2.5.2 Joint shear strain

Joint shear strains are monitored at the joint diagonals using two strain gauges as depicted in blue color in Figure 6. A simplified procedure is adopted for calculating the joint shear strain using Equation 5. This equation is a simplified version suggested in this paper which is derived based on previous study adopted by Engindeniz (Engindeniz 2008) and Hassan (Hassan et al. 2011). Engindeniz (Engindeniz 2008) calculated joint shear strain using six linear potentiometers (LP) for each external face of the joint (north face and east face). However, in this research joint shear strain is measured at the joint diagonals only using two strain gauges. Diagonal strain ( $\epsilon_{\theta_s}$ ) used in Equation 5 is the measured strain along joint diagonal. Strain values that used to plot joint response are correlated

to the diagonal that has the maximum absolute strain.  $\theta_s$  is the angle between the diagonal and the horizontal line.

$$\text{Joint shear strain } (\gamma_{sj}) = \frac{\varepsilon_{\theta_s}}{\sin \theta_s \cdot \cos \theta_s} \quad \text{Equation 5}$$

### Figure 6 Joint strain gauges

The control specimens P-1 and P-2 are designed to promote joint shear failure at which failure has happened at joint while the longitudinal reinforcement in beams and columns remained elastic. Furthermore, joint shear failure has occurred in all other specimens made with recycled concrete. Joint deformation mainly consists of diagonal joint shear strains and other strains that occur at column-joint face and beam-joint face. Strains at column-joint face and beam-joint face are very small compared to the diagonal joint shear strains because all tested specimens have failed due to joint shear without any hinges developed at joint edges. Therefore, the two strain gauges that located at the center of the joint can give reasonable prediction of joint deformation because failure has mainly occurred due to joint shear.

## 2.6 Test results and discussion

A maximum lateral load of  $\pm 55$  kN is applied to all specimens in order to compare the culminated damage under the same applied lateral loading. The lateral loading, which composed of 11 cycles, is applied at the column top of all specimens as shown in Figure 4. The behavior of test specimens is investigated in this section and the hysteresis response of the joint, which defined in terms of joint shear stress and strain, is illustrated. Strain values that used to plot joint response are correlated to the diagonal that has the maximum absolute strain and calculated using Equation 5.

### 2.6.1 Control specimens P-1 and P-2

Cylinder concrete compressive strength of the control specimens is 15 MPa. Specimens P-1 and P-2 are tested under maximum lateral loads of  $\pm 55$  kN (until cycle-11). Both specimens have experienced major diagonal shear cracks in their joint panels and some other shear cracks in their columns.

The maximum experimental joint shear stress is 7.3 MPa and the maximum joint shear strain is 0.002 rad for both specimens. The pinched hysteresis loops due to joint inclined cracking are evident. The predicted ultimate joint shear stress according to ACI 352-02 (ACI 352 2002) is 6.5 MPa which is slightly less than the maximum experimental joint shear stress. The experimental stress is recorded until cycle 11, although the specimens can sustain greater lateral loads, because the experimental program compares between the behaviors of test specimens that casted from different composite concrete materials and tested under the same level of loading. Figure 7 (a) and (b) illustrate the joint hysteresis response of the control specimens P-1 and P-2 respectively. Figure 8 (a) and (b) show the level of damage occurred in specimens P-1 and P-2 respectively until cycle 11 and clarify their crack patterns.

### **2.6.2 Specimen S-15**

Cement in specimen 15 is partially replaced by 15% of silica fume. The cylinder compressive strength of the silica fume-concrete is 24 MPa which is greater than that measured in the plain concrete (15MPa). This specimen has experienced minor diagonal shear cracks in the joint core at a maximum lateral load of  $\pm 55$  kN. The maximum experimental joint shear stress is 7.3 MPa and the maximum absolute strain for this specimen is 0.0028 rad. The predicted ultimate joint shear stress according to ACI 352-02 (ACI 352 2002) is 8.2 MPa which is slightly greater than the maximum experimental joint shear stress at cycle 11. Figure 7 (c) shows the experimental joint hysteresis response of specimen S-15 and Figure 8 (c) captures the damage occurred in this specimen till cycle 11.

### **2.6.3 Specimen S-20**

This specimen contains 20% of silica fume as partial replacement of cement in the concrete mix. The cylinder compressive strength of this material is 17 MPa. Lateral cyclic loads of  $\pm 55$  kN are applied at the top of the column. The damage occurred in this specimen is quite different than other specimens. The addition of the 20% silica fume has reduced the ductility of the specimen significantly compared to the control specimen where the maximum measured absolute strain is 0.0007 which is relatively small. Furthermore, the specimen is significantly damaged inducing diagonal shear cracks in the joint panel, minor shear cracks in the column, and column hinge at the upper part of the joint as shown in

Figure 8 (d). The joint hysteresis response of this specimen is plotted in Figure 7 (d) where the predicted ultimate joint shear stress according to ACI 352-02 (ACI 352 2002) is 6.8 MPa which is relatively close to the experimental joint shear stress at cycle 11 (7.3 MPa).

#### **2.6.4 Specimen A-15**

The cement in concrete mix of this specimen is partially replaced by 15% fuel ash. The cylinder compressive strength of the concrete-fuel ash is 31 MPa which is the highest compressive strength compared to all other test specimens. Furthermore, the maximum cumulative absolute strain of this specimen is relatively high and equals to 0.0048 which means that the addition of 15% pulverized fuel ash has increased the ductility of the specimen. The specimen has experienced large deformation under  $\pm 55$  kN lateral loads (cycle 11). The joint hysteresis response is characterized by stiffness degradation in the positive side as shown in Figure 7 (e). The predicted ultimate joint shear stress according to ACI 352-02 (ACI 352 2002) is 9.3 MPa which is greater than the experimental joint shear stress at cycle 11. This means that the specimen can sustain greater lateral loads and its experimental joint shear strength at failure can be greater than that measured at cycle 11. Minor joint shear cracks and column shear cracks have appeared in this specimen due to the applied lateral loads as shown in Figure 8 (e). This sub-assembly is relatively strong and it is slightly damaged.

#### **2.6.5 Specimen A-20**

The percentage of the fuel ash in this specimen is increased to 20% as cement partial replacement in the concrete mix. Fuel-Ash concrete (20%) has a cylinder compressive strength of 22 MPa which is less than that measured in the 15% fuel ash. This specimen is ductile and has experienced large deformation with a maximum absolute joint shear strain of 0.004 under  $\pm 55$  kN lateral loads (cycle 11). The joint hysteresis response is shown in Figure 7 (f) where the predicted ultimate joint shear stress according to ACI 352-02 (ACI 352 2002) is 7.8 MPa which is very close to the experimental joint shear stress (7.3 MPa) at cycle 11. The assembly is relatively strong and has experienced minor joint shear cracks and column shear cracks as shown in Figure 8 (f). Furthermore, spalling of the concrete cover occurred at the bottom of the column.

### 2.6.6 Specimen I-15

In this specimen 15% of the cement in the concrete mix is replaced by iron fillings at which the compressive strength of the composite concrete material is 20 MPa. The specimen is tested under  $\pm 55$  kN lateral column loads (cycle 11). The joint hysteresis response is illustrated in Figure 7 (g) with maximum experimental joint shear stress of 7.33 MPa and a maximum absolute joint shear strain of 0.0014. The addition of the 15% iron fillings has reduced the ductility of the specimen compared to the control specimen where the maximum absolute strain of the control specimen is 0.002. Figure 7 (g) shows that the predicted ultimate joint shear stress according to ACI 352-02 (ACI 352 2002), which is 7.9 MPa, is very close to the experimental joint shear stress at cycle 11. The specimen has experienced minor joint shear cracks and column shear cracks and it can still sustain higher lateral loads as shown in Figure 8 (g).

### 2.6.7 Specimen I-20

The cylinder compressive strength of concrete with 20% iron fillings, as partial replacement of cement, is 14 MPa. This specimen which has low concrete compressive strength is significantly damaged and experienced major joint shear cracks and minor column shear cracks under  $\pm 55$  kN lateral column loads (cycle 11) as shown in Figure 8 (h). The joint hysteresis response is demonstrated in Figure 7 (h) with a maximum experimental joint shear stress of 7.3 MPa and a maximum absolute strain of 0.0028 where the pinched hysteresis loops due to joint diagonal cracking are evident. Specimen I-20 (with 20% iron fillings) is more ductile than specimen I-15 (with 15% iron fillings). By contrast, the cylinder concrete compressive strength of I-20 is the least compared to all other test specimens. The predicted joint shear stress according to ACI 352-02 (ACI 352 2002) is 6.3 MPa, which is slightly less than the experimental joint shear stress at cycle 11 (7.3 MPa).

#### **Table 6 The predicted and experimental test results**

**Figure 7 Joint shear stress-strain hysteresis response of test specimens**

**Figure 8 The level of damage and crack patterns of all test specimens**

### 3. Effect of Materials

The experimental program is conducted to better understand the seismic performance of unconfined beam-column connection using composite concrete materials where cement is partially replaced by different waste materials using two different percentages 15% and 20%. Cement partial replacement with different waste materials has changed the cylinder compressive strength of concrete. Furthermore, it has significant effect on the ductility, level of damage and type of failure of test specimens.

#### 3.1 Cylinder concrete compressive strength

Regardless the type of the implemented waste material ( silica fume, pulverized fuel ash and iron fillings), the cylinder compressive strength of concrete with 15% waste material, used as cement partial replacement, is greater than that measured with 20% waste materials. Furthermore, the cylinder compressive strength of concrete with 15% pulverized fuel ash is the highest and that with 20% iron fillings is the lowest.

#### 3.2 Normalised joint shear stress

All specimens are tested under the same lateral loads of  $\pm 55$ , although the specimens can still sustain greater lateral loads, because the experimental program compares between the behaviors of test specimens that casted from different composite concrete materials and tested under the same lateral loads. Furthermore, all test specimens will be rehabilitated and tested under full loads in future work. The normalized joint shear stress can give best indication for joint response because the compressive strength of test specimens varies based on the type and percentage of the implemented waste material. Figure 9 illustrates the joint hysteresis response of all test specimens defined in terms of normalized joint shear stress and joint shear strain. The normalized joint shear stress of the control specimen, which is almost 2, is the greatest value compared to all test specimens while the normalized joint stress of specimen A-15 is 1.3 and is the least. This means that the control specimen is damaged and stressed significantly inside the joint panel while specimen A-15 is not under the same applied later

loads. Control specimen is significantly damaged under the applied lateral loads but A-15 can still sustain higher loads and is not significantly damaged. Therefore, the normalized joint shear stress of the control beam illustrated in Figure 9 (a and b) is greater than the predicted normalized ultimate stress while that in specimen A-15 is less than the predicted and hence specimen A-15 can still sustain greater lateral loads.

### 3.3 Ductility

Ductility is an important factor for any structural element under seismic loads. Joint shear strains provide an approximate prediction of joint ductility where beam-column connections that fail under low shear strains are less ductile than those that fail under high joint shear strains.

Cement partial replacement with waste material has significant influence on the shear strains of beam-column connection tested under cyclic loading. Specimen A-15 which contains 15% pulverized fuel ash has experienced a maximum absolute strain of 0.0048 under  $\pm 55$  lateral loads which is the highest value compared to all test specimens. By contrast, joint shear strain of specimen S-20 that contains 20% silica fume is the lowest (0.00078). Joint shear strain of the control specimen is 0.002. Pulverized fuel ash concrete has increased the ductility of the joint while 20% of silica-fume concrete has decreased its ductility. Joint shear strains of all test specimens are listed in Table 6.

Joint shear strains of specimen S-20 and specimen I-15 are less than that measured in the control specimen indicating that the ductility of specimen S-20 and I-15 is less than that found in control specimen. This has happened due to the variation in material properties of the specimens. The ultimate cylindrical compressive strains of specimen P-1, S-20 and I-15 are 0.016, 0.008 and 0.012 respectively and the ultimate cylindrical tensile strains of the same specimens are 0.00165, 0.00081 and 0.00123 respectively as shown in Table 4 and Table 5. The cylindrical compressive and tensile strains of all other specimens are greater than that measured in the control specimen as shown in Table 4 and Table 5. This explains the reduction in the ductility measured in specimen I-15 and S-20.



### 3.4 Level of damage

Specimens with low concrete compressive strength such as P-1 ,P-2 ,I-20 and S-20 are significantly damaged under the  $\pm 55$  imposed lateral loads while other specimens (A-15, A-20, I-15 and S-15) are stronger and have experienced minor shear cracks with small crack width. Specimen A-15, which has 15 % pulverised fuel ash as cement partial replacement and has the highest concrete compressive strength, is the strongest specimen and the least damaged one. Figure 10 illustrates the level of damage in each specimen where the red colour depicts cracks that appear in pulling cycles and the blue colour depicts cracks that appeared in pushing cycle. Pushing and pulling directions are shown in Figure 4. The symbols shown on the joints' images in Figure 10 denote the cycle number followed by the magnitude of lateral load at which the crack appeared. ie 'C-1, 24' means cycle number 1 where crack appeared at a lateral load of 24 kN. Joints Cracks pattern shown in Figure 10 are depicted at the front face of the joint while the strain gauges instrumented at the rare face.

**Figure 9 The normalised joint shear stress vs joint shear strain for test specimens.**

**Figure 10 The level of damage and crack pattern of test specimens.**

## 4. Conclusions

A series of cyclic tests on unconfined beam-column connections with different concrete mixes are conducted in this research. Cement in concrete mixes is partially replaced by different waste materials (Pulverized fuel ash, silica fume and iron fillings) using two different percentages 15% and 20%. Based on the experimental study, the following points are observed:

1. Cement partial replacement with different waste materials has changed the cylinder compressive strength of concrete. Furthermore, it has significant effect on the ductility, level of damage and type of failure of test specimens.
2. Regardless the type of the implemented waste material ( silica fume, pulverized fuel ash and iron fillings), the cylinder compressive strength of concrete with 15% waste material, used as cement partial replacement, is greater than that measured with 20% waste materials.

3. The cylinder compressive strength of concrete with 15% pulverized fuel ash is the highest and that with 20% iron fillings is the lowest.
4. The normalized joint shear stress of the control specimen is the highest compared to all test specimens while the normalized joint stress of specimen A-15 is the lowest. This means that the control specimen is damaged and stressed significantly inside the joint panel while specimen A-15 is not under the same applied later loads.
5. The maximum ultimate joint shear strain of specimen A-15 is 0.0048 which is almost double that measured in the control specimen (0.002) while the maximum ultimate joint shear strain of specimen S-20 is 0.00078 which is less than half that measured in control specimen. This means that pulverized fuel ash concrete has increased the ductility of joint under seismic loading while the 20% of silica-fume concrete has decreased its ductility.
6. Specimens with low concrete compressive strength such as P-1, P-2, I-20 and S-20 are significantly damaged under the  $\pm 55$  imposed lateral loads while other specimens (A-15, A-20, I-15 and S-15), with a relatively high compressive strength, are stronger and have experienced minor shear cracks with small cracks width.
7. The proper partial replacement percentage of cement is found 15% for the Pulverized fuel ash, silica fume and iron fillings. Increasing this percentage to 20% tends to decrease the concrete cylinder compressive strength.
8. It is recommended using pulverized fuel ash in order to enhance the performance of beam-column connection under cyclic loading. The pulverized fuel ash-concrete increases the ductility of RC beam column-connection and reduces its damage level and crack width which means that the specimen can still sustain higher lateral loads.
9. Silica fume and iron filling are also recommended and can enhance the joint behavior under cyclic loading but the enhancement is most remarkable when using 15% of pulverized fuel ash.
10. The level of damage, joint shear strain and mode of failure are significantly influenced by the type and percentage of the implemented waste material.
11. It is recommended to recycle some waste materials such as pulverized fuel ash, silica fume and iron fillings in concrete mix to reduce environmental pollution and to enhance concrete mixes.

## 5. Acknowledgment

Financial assistance provided by King Abdullah II Design and Development Bureau (KADDB) is greatly appreciated. The testing frame rig provided by Jordan University of Science and Technology through Prof. Ghazi abu Farsakh is highly acknowledged.

## 6. References

- 1 Alzaed, Ali N. 2014. "Effect of Iron Filings in Concrete Compression and Tensile Strength." *International Journal of Recent Development in Engineering and Technology* 3 (4).
- 2 Dhir, R K, JGL Munday, and L T Ong. 1984. "INVESTIGATIONS OF THE ENGINEERING PROPERTIES OF OPC/PULVERISED FUEL ASH CONCRETE: STRENGTH DEVELOPMENT AND MATURITY" 77 (June).
- 3 Engindeniz, Murat. 2008. "Repair and Strengthening of Pre-1970 Reinforced Concrete Corner Beam-Column Joints Using CFRP Composites," May. Georgia Institute of Technology.
- 4 Hassan, Wael Mohammed, and Wael Mohammed. 2011. "Analytical and Experimental Assessment of Seismic Vulnerability of Beam-Column Joints without Transverse Reinforcement in Concrete Buildings." *ProQuest Dissertations And Theses; Thesis (Ph.D.)--University of California, Berkeley, 2011.; Publication Number: AAT 3473895; ISBN: 9781124889542; Source: Dissertation Abstracts International, Volume: 72-12, Section: B, Page: 7544.; 499 P.*
- 5 Khedr, Safwan A., and Mohamed Nagib Abou-Zeid. 1994. "Characteristics of Silica-Fume Concrete." *Journal of Materials in Civil Engineering* 6 (3): 357–75. [https://doi.org/10.1061/\(ASCE\)0899-1561\(1994\)6:3\(357\)](https://doi.org/10.1061/(ASCE)0899-1561(1994)6:3(357)).
- 6 Lam, L, Y.L Wong, and C.S Poon. 1998. "Effect of Fly Ash and Silica Fume on Compressive and Fracture Behaviors of Concrete." *Cement and Concrete Research* 28 (2). Pergamon: 271–83. [https://doi.org/10.1016/S0008-8846\(97\)00269-X](https://doi.org/10.1016/S0008-8846(97)00269-X).
- 7 Liu, Miao. 2010. "Self-Compacting Concrete with Different Levels of Pulverized Fuel Ash." *Construction and Building Materials* 24 (7): 1245–52. <https://doi.org/10.1016/j.conbuildmat.2009.12.012>.
- 8 M-Gharrib Noori, Krikar, and Hawkar Hashim Ibrahim. 2018. "MECHANICAL PROPERTIES OF CONCRETE USING IRON WASTE AS A PARTIAL REPLACEMENT OF SAND." <https://doi.org/10.23918/iec2018.16>.
- 9 Matsumoto, T, H Nishihara, M Nakao, and J J Castro. 2012. "Experimental Study on Shear Strength of Eccentric Beam-Column Joints Subjected to Seismic Loading in Super High Rise Reinforced Concrete Buildings." [http://www.iitk.ac.in/nicee/wcee/article/WCEE2012\\_1035.pdf](http://www.iitk.ac.in/nicee/wcee/article/WCEE2012_1035.pdf).
- 10 Murad, Yasmin Zuhair. 2016. "Analytical and Numerical Assessment of Seismically Vulnerable Corner Connections under Bidirectional Loading in RC Framed Structures." *ProQuest Dissertations And Theses; Thesis (Ph.D.)--Imperial College London, London, 2016.* Imperial College London. <https://spiral.imperial.ac.uk/handle/10044/1/44493>.
- 11 Pampanin, S., G.M. Calvi, and M. Moratti. 2002. "Seismic Behavior of R.C. Beam-Column Joints Designed for Gravity Only." University of Canterbury. Civil Engineering. <https://ir.canterbury.ac.nz/handle/10092/173>.
- 12 Paulay, T, and M J N Priestley. 1992. "SEISMIC DESIGN OF REINFORCED CONCRETE AND MASONRY BUILDINGS."
- 13 "Recommendations for Design of Beam-Column Connections in Monolithic Reinforced Concrete Structures." 2002. [http://civilwares.free.fr/ACI/MCP04/352r\\_02.PDF](http://civilwares.free.fr/ACI/MCP04/352r_02.PDF).

## 7. List of tables

Table 1 Plane and recycled concrete mixing ratios .....	6
Table 2 Chemical composition of the implemented waste materials. ....	7
Table 3 Properties of the waste materials .....	7
Table 4 Specimens' compressive behaviour.....	8
Table 5 Specimens' tensile behaviour .....	8
Table 6 The predicted and experimental test results.....	17

## 8. List of figures

Figure 1 joint shear failure (Pampanin, Calvi, and Moratti 2002).....	5
Figure 2 Test specimen details.....	9
Figure 3 Test setup.....	9
Figure 4 (a) Specimens constraints and (b) lateral load pattern .....	10
Figure 5 Strain gauges location .....	11
Figure 6 Joint strain gauges .....	13
Figure 7 Joint shear stress-strain hysteresis response of test specimens .....	18
Figure 8 The level of damage and crack patterns of all test specimens.....	19
Figure 9 The normalised joint shear stress vs joint shear strain for test specimens. ....	23
Figure 10 The level of damage and crack pattern of test specimens. ....	24

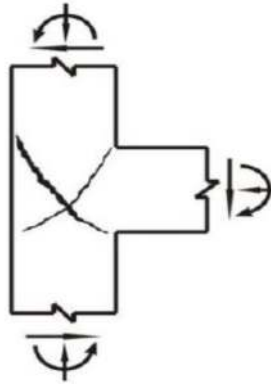


**Figure 1 joint shear failure (Pampanin, Calvi, and Moratti 2002)**

Draft

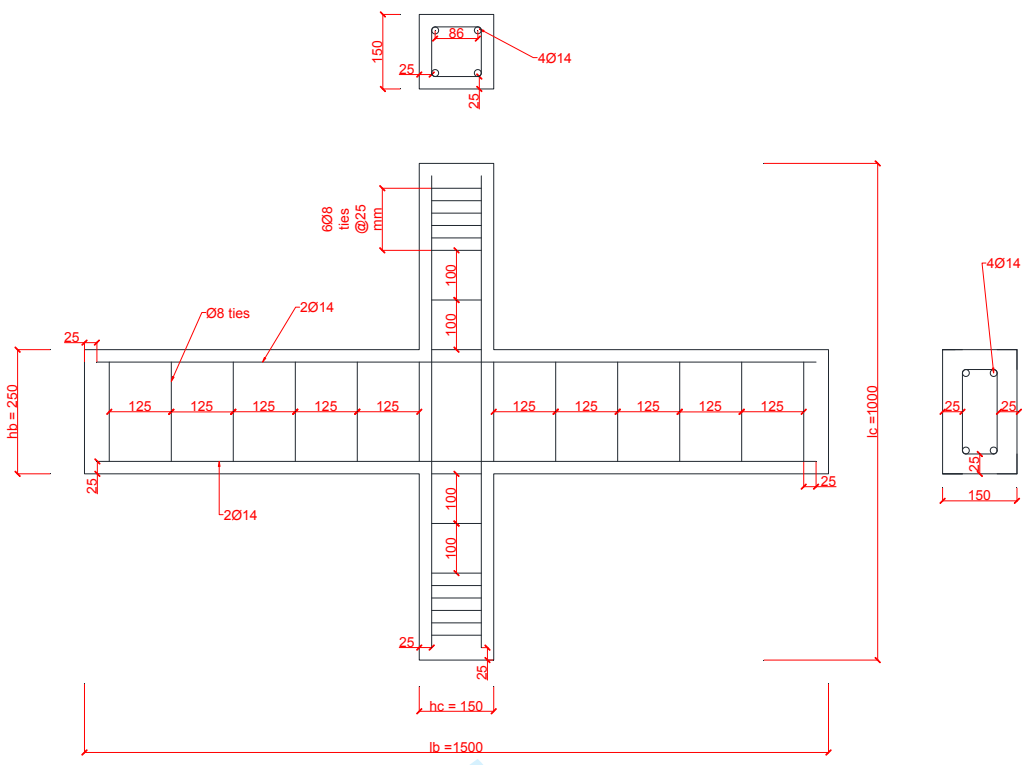
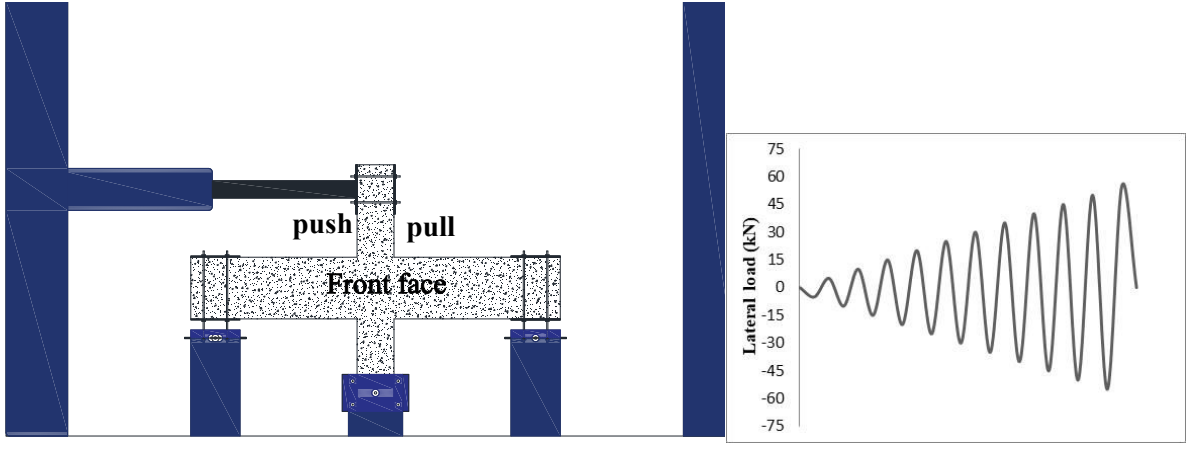


Figure 1 Test specimen details



**Figure 1 Test setup**

Draft



(a) (b)  
Figure 1 (a) Specimens constraints and (b) lateral load pattern

Draft





**Figure 1 Strain gauges location**

Draft

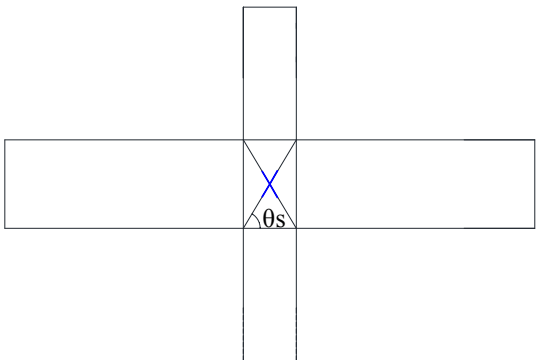


**Figure 1 Joint strain gauges**

Draft

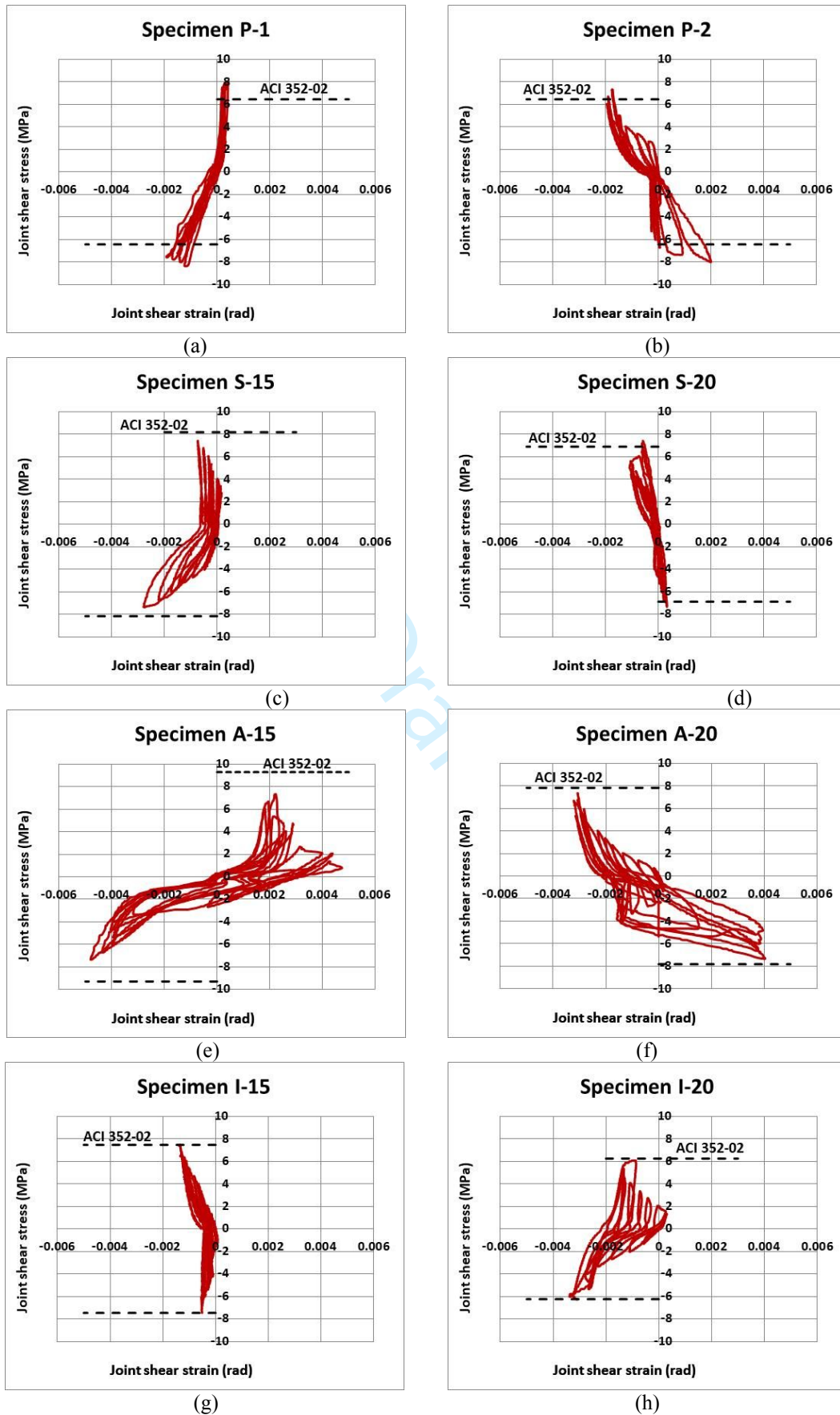


Figure 1 Joint shear stress-strain hysteresis response of test specimens



**Figure 1** The level of damage and crack patterns of all test specimens

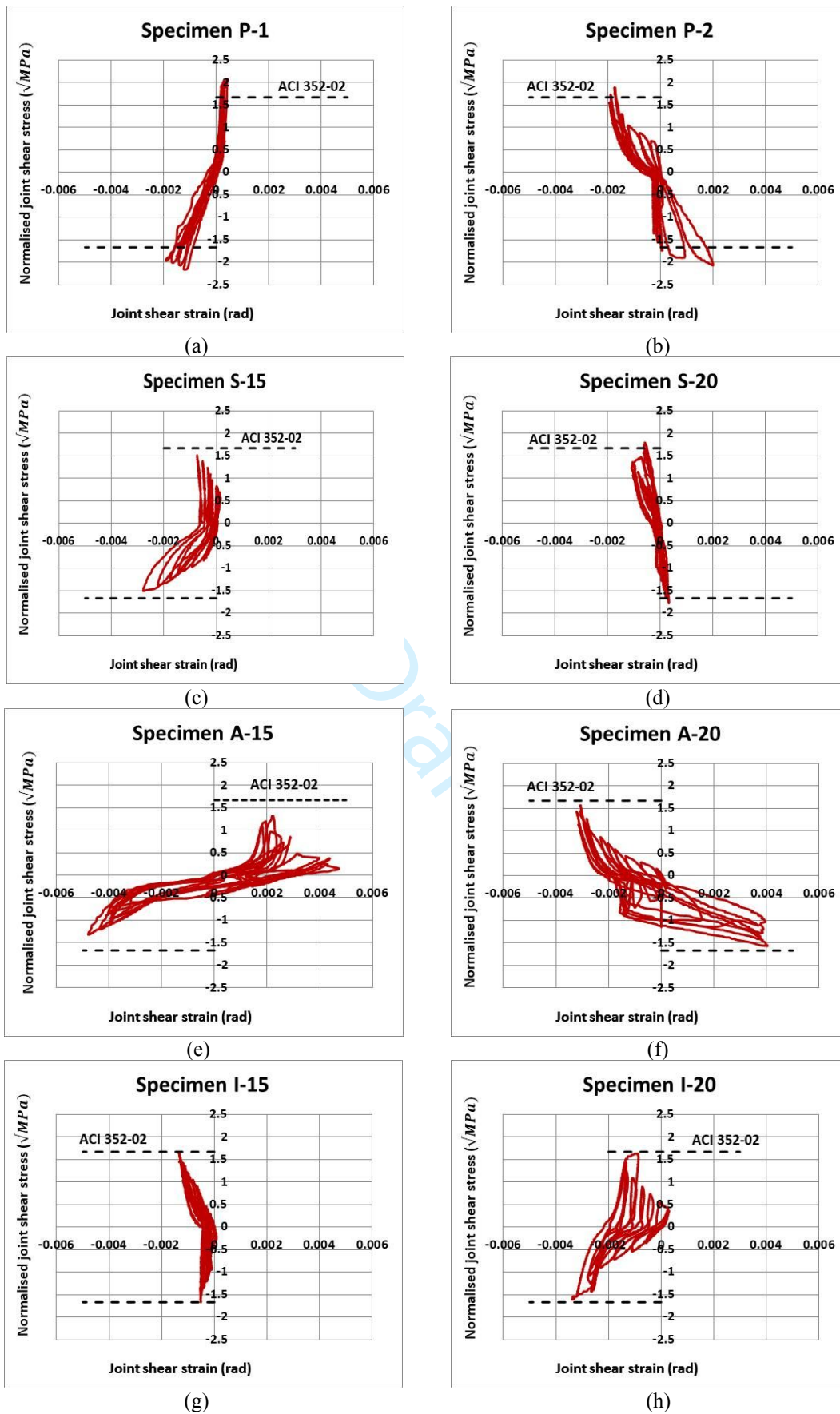
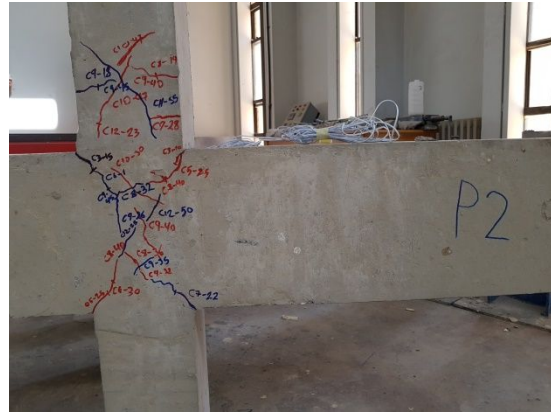


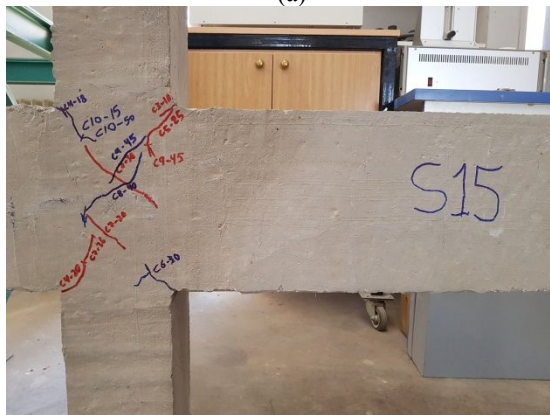
Figure 1 The normalised joint shear stress vs joint shear strain for test specimens.



(a)



(b)



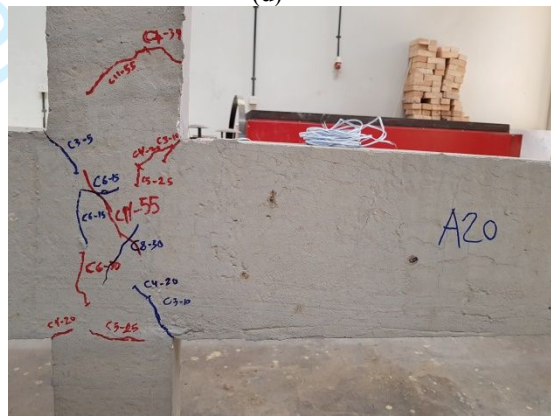
(c)



(d)



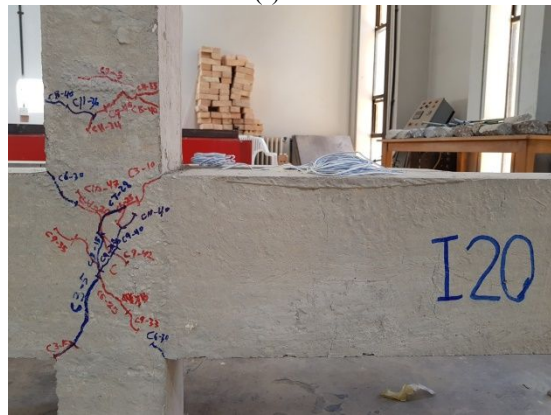
(e)



(f)



(g)



(h)

Figure 1 The level of damage and crack pattern of test specimens.

**Table 1** Plane and recycled concrete mixing ratios

<b>Mixture</b>	<b>Cement (kg/m<sup>3</sup>)</b>	<b>Waste material Type</b>	<b>Waste material (kg/m<sup>3</sup>)</b>	<b>Sand (kg/m<sup>3</sup>)</b>	<b>Fine aggregate (kg/m<sup>3</sup>)</b>	<b>Coarse aggregate (kg/m<sup>3</sup>)</b>	<b>Water/cement ratio</b>
<b>P1,P2</b>	401	/	0	742	636	623	0.6
<b>A-15</b>	350	Pulverised fuel Ash	52.5	742	636	623	0.6
<b>A-20</b>	333	Pulverised fuel Ash	68.0	742	636	623	0.6
<b>I-15</b>	350	Iron filings	52.5	742	636	623	0.6
<b>I-20</b>	333	Iron filings	68.0	742	636	623	0.6
<b>S-15</b>	350	Silica fume	52.5	742	636	623	0.6
<b>S-20</b>	333	Silica fume	68.0	742	636	623	0.6

Draft

**Table 1** Chemical composition of the implemented waste materials.

Oxides (%)	Pulverised fuel ash	Silica fume	Iron filings
H <sub>2</sub> O	0.06	0.46	-
SiO <sub>2</sub>	62.52	92.98	-
Al <sub>2</sub> O <sub>3</sub>	24.65	0.49	-
Fe <sub>2</sub> O <sub>3</sub>	4.79	1.49	-
TiO <sub>2</sub>	1.16	-	-
CaO	2.23	0.32	-
MgO	1.19	0.57	-
SO <sub>3</sub>	0.31	0.57	-
K <sub>2</sub> O	-	0.51	-
Na <sub>2</sub> O	-	0.47	-
Cl	-	0.04	-
LOI	-	1.8	-
LOI on 500°C	0.69	-	-
LOI on 750°C	0.88	-	-
LOI on 950°C	0.91	-	-
C	-	-	3.53
Si	-	-	2.67
Mg	-	-	0.05
S	-	-	0.01
P	-	-	0.03
Mn	-	-	0.31
Fe	-	-	93.4
+ 45 Micron Sieve analysis	19.60	-	-
Residual coarse particle (+0.045 in diameter 0.1 max)	-	0.94	-



**Table 1 Properties of the waste materials**

<b>Material Properties</b>	<b>Silica fume</b>	<b>Iron filling</b>	<b>Pulverised fuel ash</b>
<b>Density (g/cm<sup>3</sup>)</b>	1.5 – 2	2.88	1.1 - 1.7
<b>Solubility in water</b>	Nearly insoluble	Insoluble	Insoluble ( <2% )
<b>Explosion hazard</b>	Hazardous	Slight	No hazard

Draft

**Table 1 Specimens' compressive behaviour**

<b>Specimen</b>	<b>Cement partial replacement (%)</b>	<b>Concrete compressive strength (<math>f'_c</math>) (MPa)</b>	<b>Strain at maximum compressive strength</b>	<b>Ultimate compressive strain</b>	<b>Modulus of elasticity (MPa)</b>
<b>P-1</b>	0	15	0.01	0.016	16667
<b>P-2</b>	0	15	0.01	0.016	16667
<b>S-15</b>	15	24	0.0075	0.0216	4166
<b>S-20</b>	20	17	0.0015	0.008	15000
<b>A-15</b>	15	31	0.005	0.036	6200
<b>A-20</b>	20	22	0.006	0.032	3667
<b>I-15</b>	15	20	0.0075	0.012	3000
<b>I-20</b>	20	14	0.0075	0.024	2000

Draft

**Table 1 Specimens' tensile behaviour**

<b>Specimen</b>	<b>Cement partial replacement (%)</b>	<b>Concrete tensile strength (<math>f_t</math>) (MPa)</b>	<b>Strain at maximum tensile strength</b>	<b>Ultimate tensile strain</b>
<b>P-1</b>	0	1.45	0.00028	0.00165
<b>P-2</b>	0	1.45	0.00028	0.00165
<b>S-15</b>	15	2.35	0.00035	0.00220
<b>S-20</b>	20	1.67	0.00012	0.000810
<b>A-15</b>	15	3.00	0.00060	0.00360
<b>A-20</b>	20	2.22	0.00050	0.00315
<b>I-15</b>	15	2.00	0.00020	0.00123
<b>I-20</b>	20	1.45	0.00050	0.00245

Draft

Table 1 The predicted and experimental test results

Specimen	Concrete compressive strength ( $f'_c$ ) (MPa)	Predicted Joint shear strength (kN)	Experimental joint shear force (kN)	Experimental Joint shear stress (MPa)	Normalised Experimental joint shear stress ( $\sqrt{MPa}$ )	Absolute ultimate shear strain (rad)
P-1	15	145.53	165	7.33	1.89	0.0019
P-2	15	145.53	165	7.33	1.89	0.002
S-15	24	184.08	165	7.33	1.51	0.0028
S-20	17	154.93	165	7.33	1.79	0.00078
A-15	31	209.21	165	7.33	1.32	0.0048
A-20	22	176.24	165	7.33	1.57	0.004
I-15	20	168.04	165	7.33	1.67	0.0014
I-20	14	140.59	165	7.33	1.62	0.0028

Draft